

# Supplementary Information for “Impact of noise on landscapes metrics generated with Stream Power models”

Matthew J. Morris<sup>1</sup> and Gareth G. Roberts<sup>1</sup>

<sup>1</sup>Department of Earth Science and Engineering, Imperial College London, Royal School of Mines, South Kensington, London, SW7 2AZ, UK

**Correspondence:** Matthew J. Morris (matthew.morris15@imperial.ac.uk)

## S1 Summary

This Supplementary Information document contains 11 figures, extending the results presented in the main manuscript. Figure S1 shows the distributions of noisy functions added to topography in scenarios A–D. Figures S2 and S3 show examples of ‘square’, ‘escarpment’ and ‘domal’ landscapes and planform geometries generated using the same procedures and parametrisations as those presented in the main manuscript but with no inserted noise. Figure S4 shows impact of assumed value of concavity index on uplift rates estimated from  $\chi$ -analysis. Figure S5 demonstrates how changing the amplitude of noise in the starting condition affects the recovery of  $\theta$  and  $U$  from slope-area analysis, and affects  $z(\chi)$  profiles. Figure S6 shows maps of drainage location probabilities for 100 simulations of red, white, and blue noise added to scenarios A–C. Figures S7 and S8 show assessment of steady state for landscapes generated with quenched and spatio-temporal noise. Figures S9–S11 show impact of inserting un-eroded white, blue and red noise on calculated metrics for select landscapes. All of these results are discussed in the main manuscript.

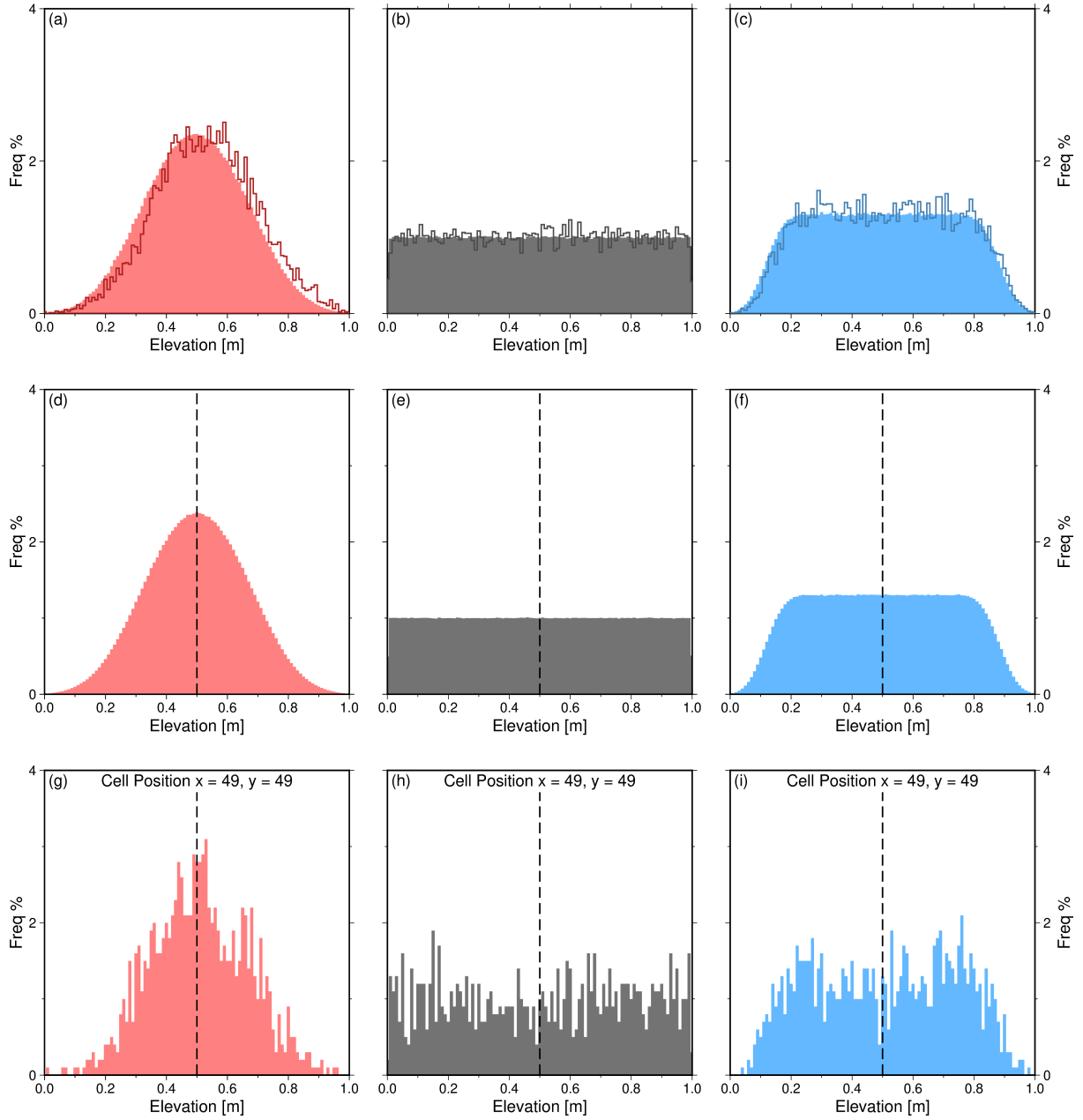


**Figure S1. Verifying the distributions of noisy functions added to landscapes** (a–c) Filled histograms = distributions of elevations for 100 different noisy functions of red, white, and blue noise respectively. Solid lines = distributions of a elevations for a single simulation. These noisy functions are used as initial conditions in scenarios A–D, as quenched noise in scenario B, and as final noise in Scenario (D), where they are scaled by  $\alpha = 2, 20$ , and  $200$ . (d–f) Distributions of red, white, and blue spatio-temporal noise used for a single simulation within scenario C, for all grid cells. (g–i) As above, for a single grid cell within the same simulation.

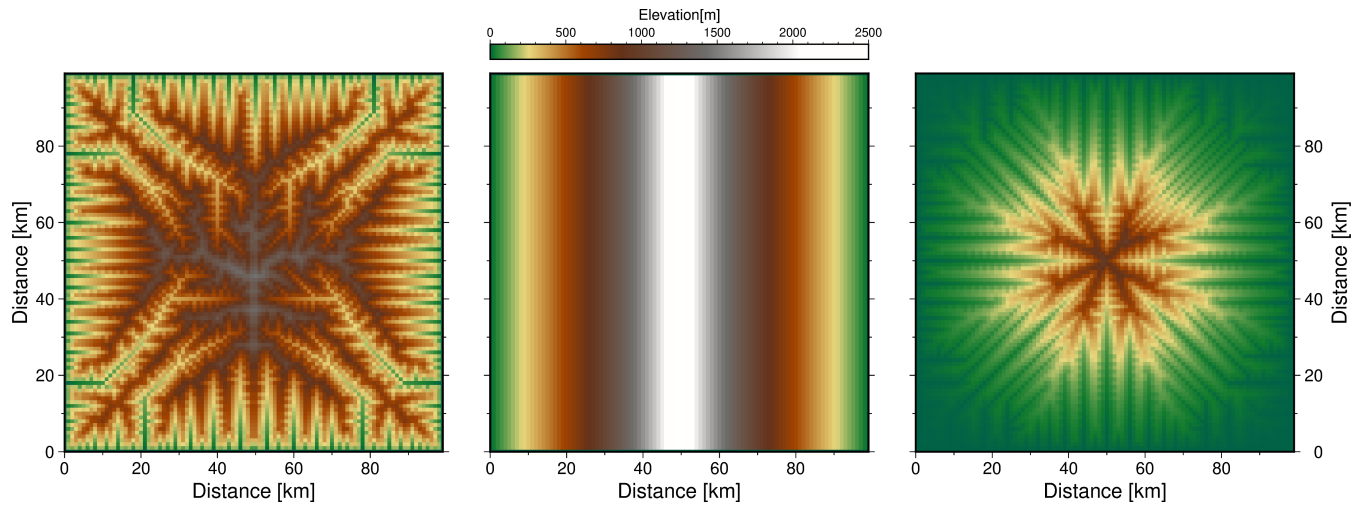


**Figure S2. Landscapes without inserted noise.** (a) ‘Square’, (b) ‘escarpment’ and (c) ‘domal’ landscapes produced as described in the main manuscript but without added noise.

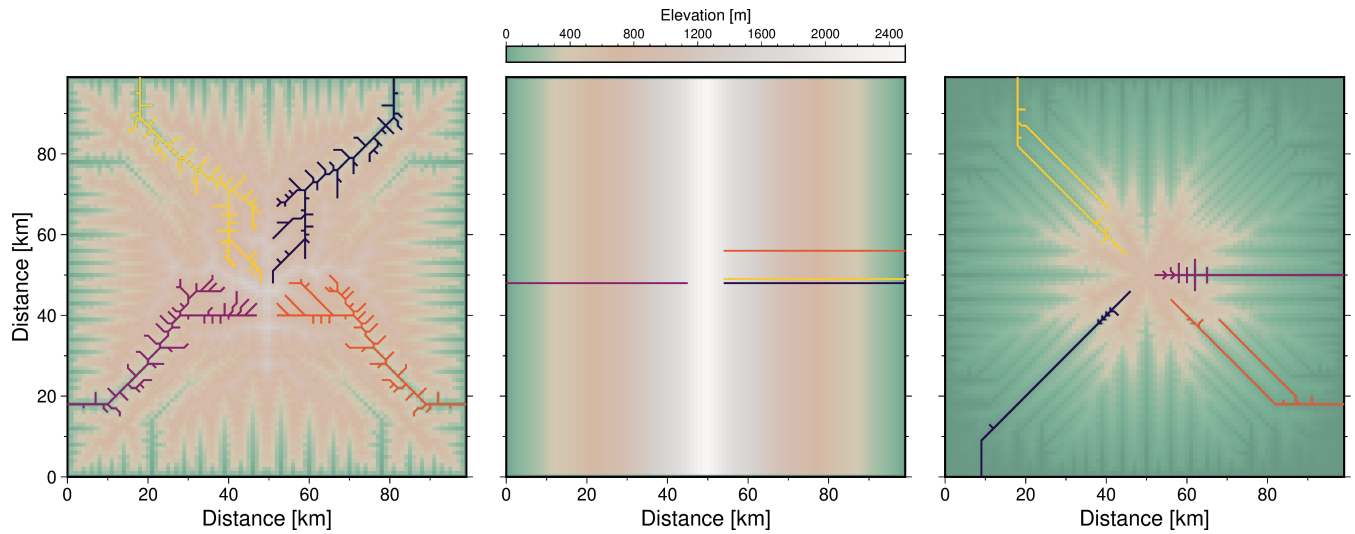


**Figure S3. Planforms of drainage networks in landscapes without inserted noise.** Coloured lines = four largest drainage networks within the (a) ‘square’, (b) ‘escarpment’ and (c) ‘domal’ landscapes shown in Figure S2 of this document.

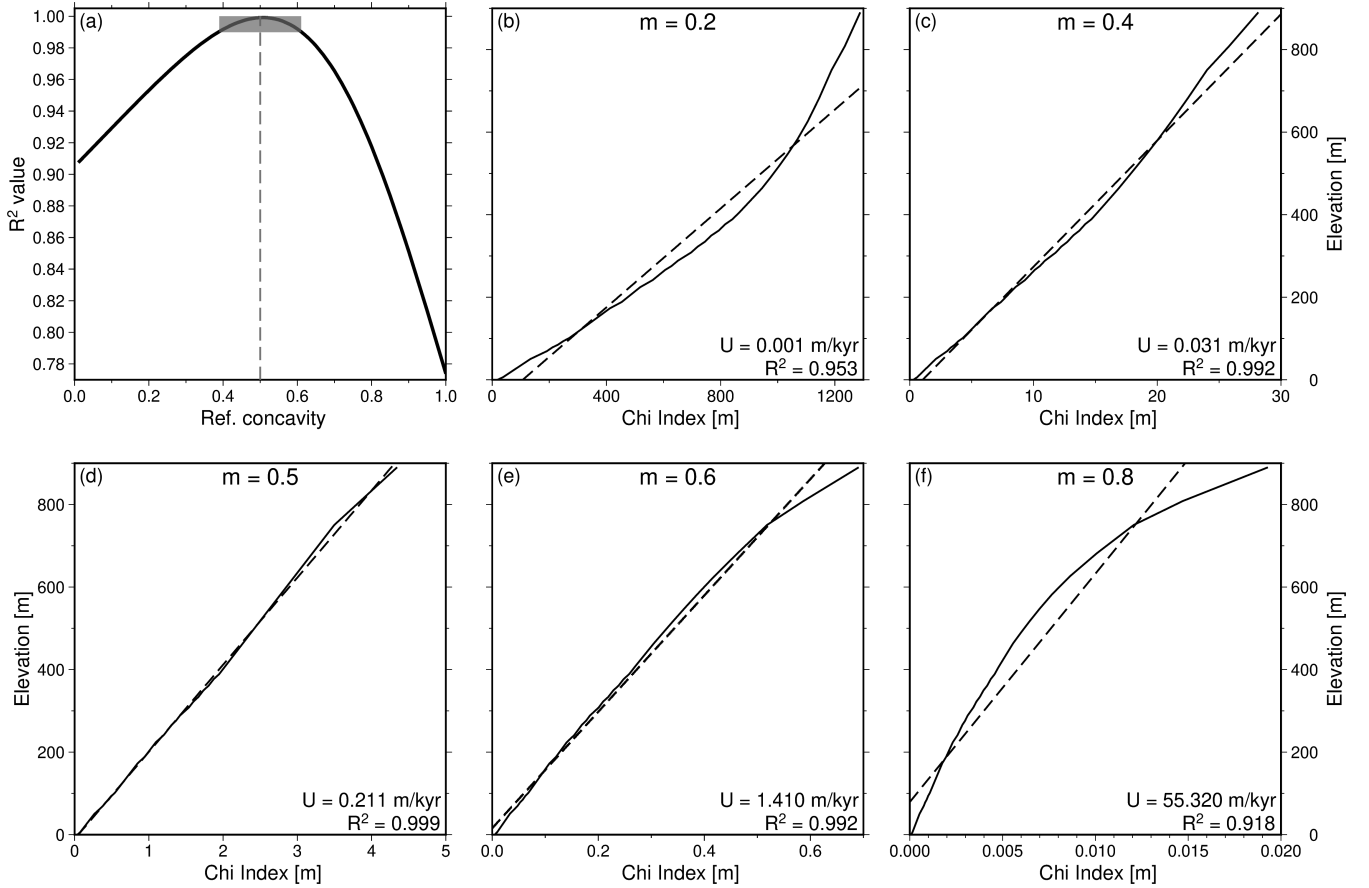


**Figure S4. Impact of assumed value of concavity index on recovery of uplift rates from chi-analyses.** Chi-analysis of longest river extracted from a steady landscape (at 100 Myr) generated with white noise only in the initial condition (from catchment coloured yellow in Figures 6b and 10d in the main manuscript). (a) Black curve = results from linear regression of chi-elevation data generated with annotated values of concavity index ( $\theta = m/n$ ); dashed line = true value used to generate the synthetic landscape; grey band = values where  $R^2 > 0.99$ . (b–f) Examples of chi-elevation profiles (solid line) used to generate the solid curve in panel (a) with annotated values of  $m$  (note,  $n = 1$ , hence  $\theta = m$ ). Dashed line = linear regression; note annotated  $R^2$  values and recovered uplift rates (see Equation 19 in the main manuscript).

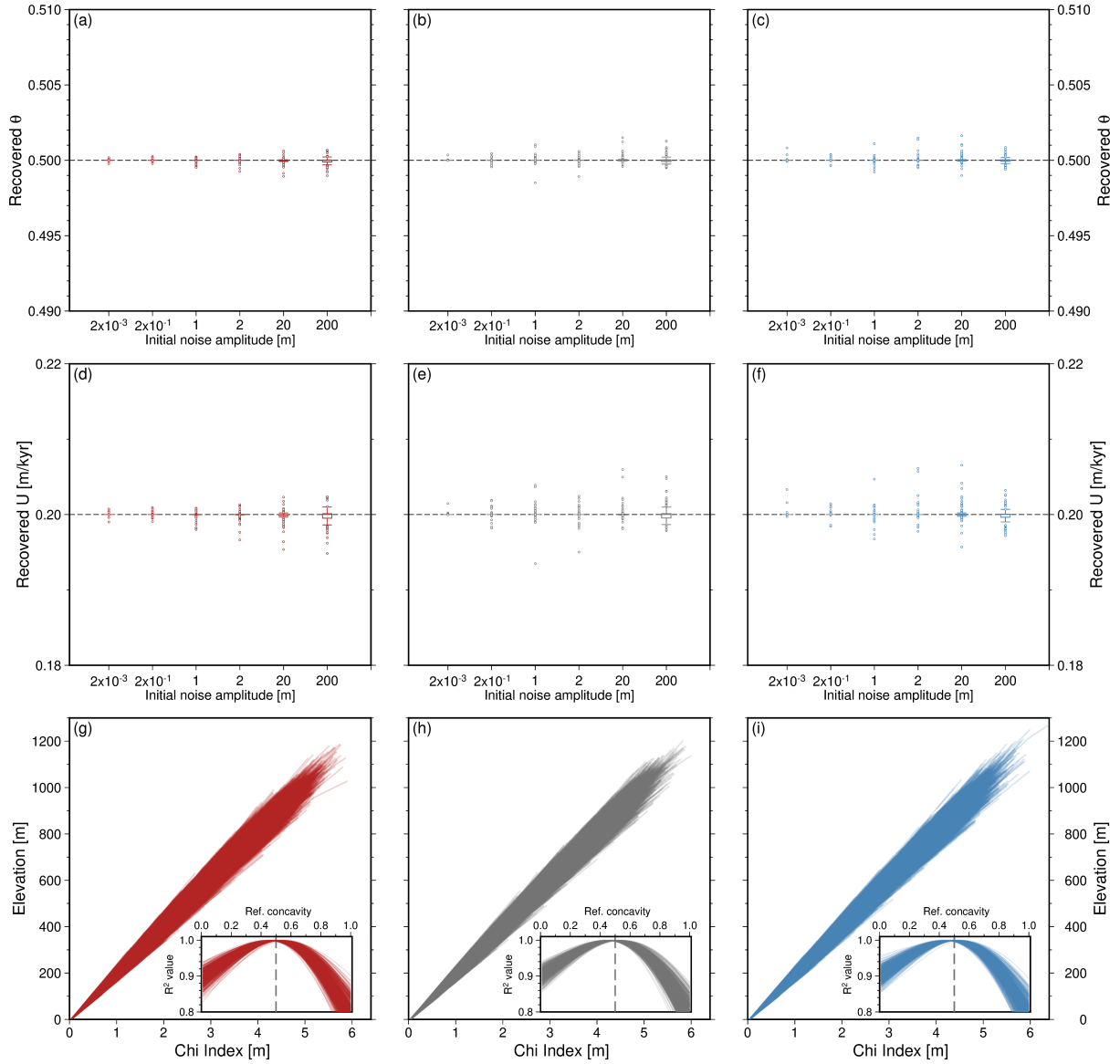


**Figure S5. Impact of amplitude of initial red, white or blue noise on geomorphic metrics recovered from steady state ‘square’ landscapes.** (a–f) Each box-and-whiskers plot shows results for  $M = 100$  landscapes generated with annotated initial noise of indicated colour. Whiskers =  $1.5 \times \text{IQR}$ , or maxima/minima if higher/lower; dots = fliers. (a–c) Range of  $\theta$  values recovered from slope-area analysis. Dashed black line shows ‘true’  $\theta$  value used to parametrise LEM. (d–f) Range of uplift rates recovered from slope-area analysis. (g–i)  $\chi$ -elevation profiles and associated reference concavities for all channels in the largest basin in each simulation with the different amplitudes of noise indicated in panels (a–f).

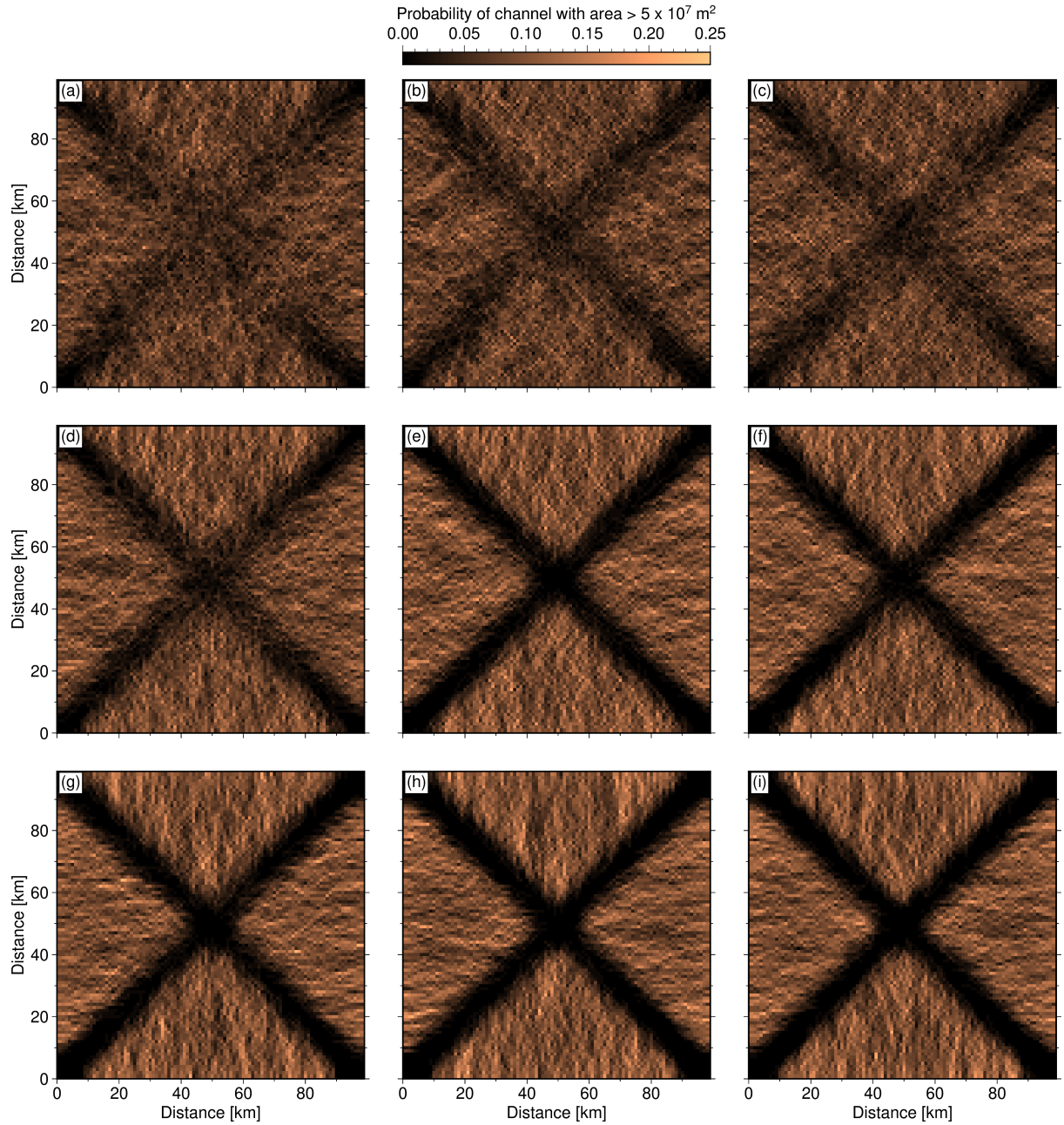


**Figure S6. Probability of drainage within landscapes generated by 100 different arrangements of initial, quenched, and spatio-temporal noise.** (a–c) Colours indicate probability of a grid cell in 100 ‘square’ landscapes containing a channel with upstream drainage area  $> 5 \times 10^7 \text{ m}^2$  generated with initial red (a), white (b), or blue (c) noise. Compare to the equivalent panels in Figure 8a–c of the main manuscript for 1000 simulations, demonstrating convergence from 100 simulations. (d–f) As above, for landscapes containing quenched noise, and (g–i) for landscapes with spatio-temporal noise added. Examples of landscapes with white quenched or spatio-temporal noise added are shown in Figures 17a and 18a.

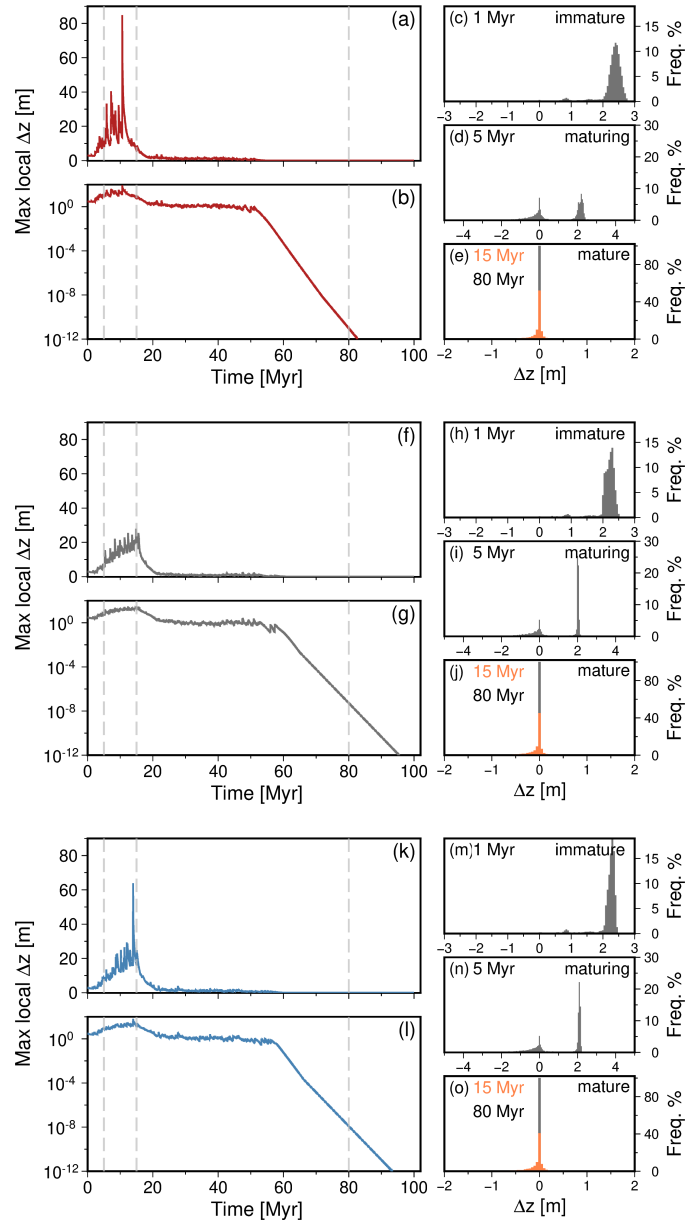


**Figure S7. Identifying steady state landscapes with quenched noise.** In each of these examples the same arrangement of red (a–e), white (f–j) or blue (k–o) noise is inserted at each time step into ‘square’ landscapes. See scenario B in Figure 3 of the main manuscript. (a) Evolution of maximum change in local elevation ( $\Delta z_\alpha$ ) between consecutive time steps ( $\Delta t = 0.01$  Ma; see Equation 9 in main manuscript). Grey dashed vertical lines correspond to histograms shown in panels (c)–(e). (c) Histogram of elevation change,  $\Delta z$ , for all grid cells between 0.99 and 1 Myr. (d) & (e) As per (c), from 4.99  $\rightarrow$  5 Myr, 14.99  $\rightarrow$  15 Myr and 79.99  $\rightarrow$  80 Myr, respectively. (f–j) As above for white noise. (k–o) As above for blue noise.

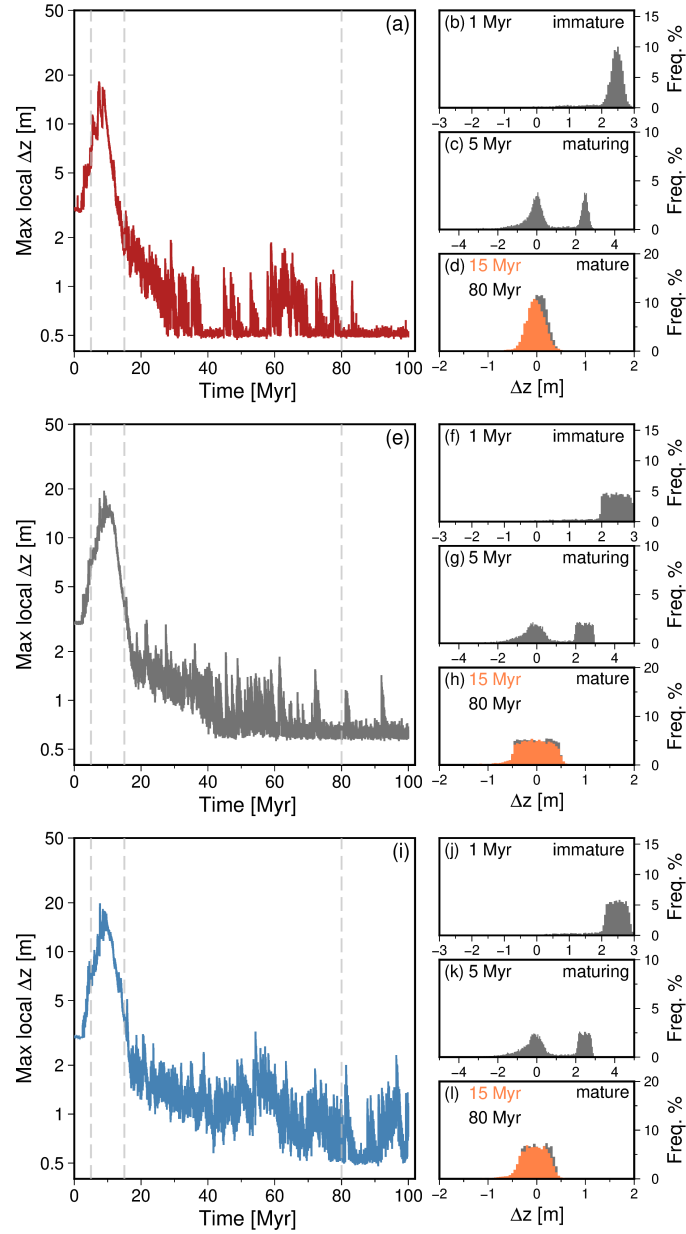


**Figure S8. Identifying steady state landscapes with spatio-temporal noise (scenario C).** In each of these examples the same distribution but different arrangements of red (a–d), white (e–h) or blue (i–l) noise is inserted at each time step into ‘square’ landscapes. See Figure S7 for extended description.



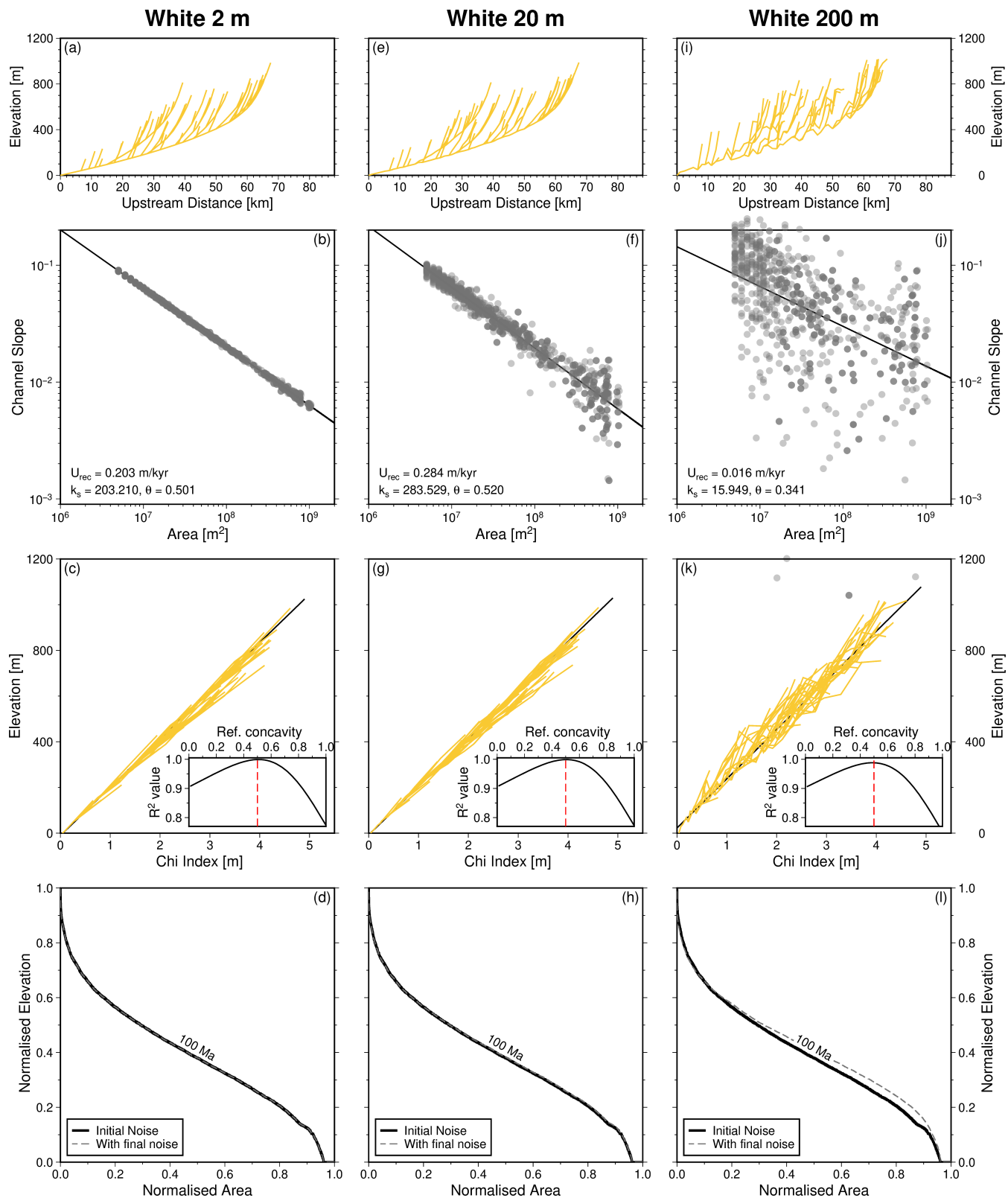


**Figure S9. Examples of geometries of river profiles and associated metrics in landscapes with un-eroded white noise.** (a–d) Results when up to 2 m of un-eroded noise is added to steady state landscape shown in Figure 6e of the main manuscript (see Figures 18–19 of main manuscript). (a) Longitudinal profiles of rivers extracted from largest basin. (b) Gray circles = slope-area analysis and associated metrics of the longest river. Note: some measurements extend beyond panel bounds in later examples with higher amplitude noise. Black line = linear regression; associated values of  $\theta$ ,  $k_s$  and  $U_{rec}$  are annotated. True uplift rate = 0.2 m/kyr, and  $\theta = 0.5$ . (c) Chi-elevation profiles of rivers shown in panel (a). Black line = linear regression. Inset shows  $R^2$  values for different concavity indices used to linearise river profiles; red dashed line = true value used to produce the landscape. (d) Hypsometry of steady state landscapes with only initial noise (solid) and with additional (un-eroded) noise (dashed; cf. Figures 18a and 18b in main manuscript). (e–h) and (i–l) Results when up to 20 and 200 m of un-eroded noise are incorporated, respectively.

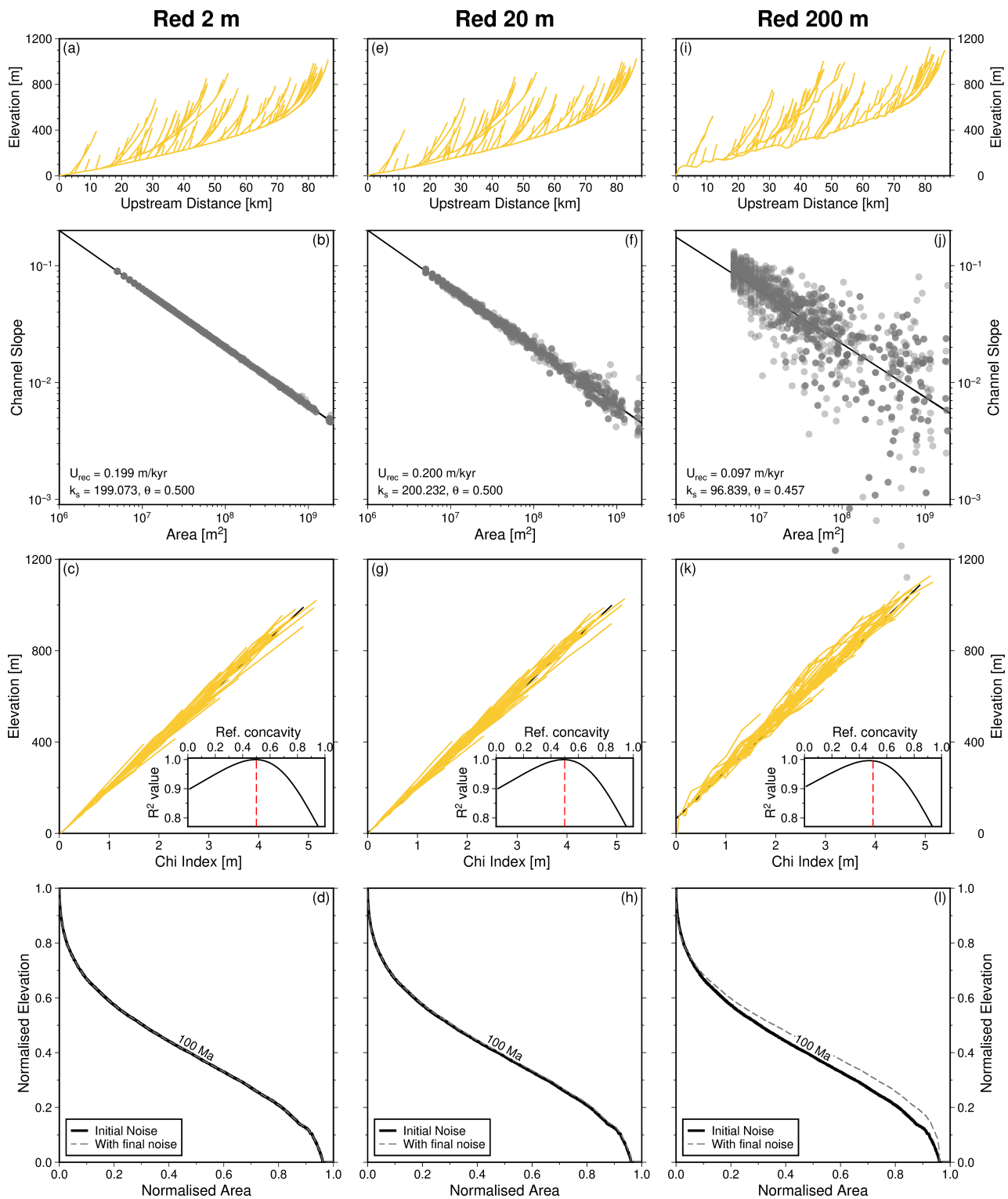


**Figure S10. Geometries of river profiles and associated metrics generated with un-eroded red noise.** (a–j) See caption to Figure S9 for extended description.

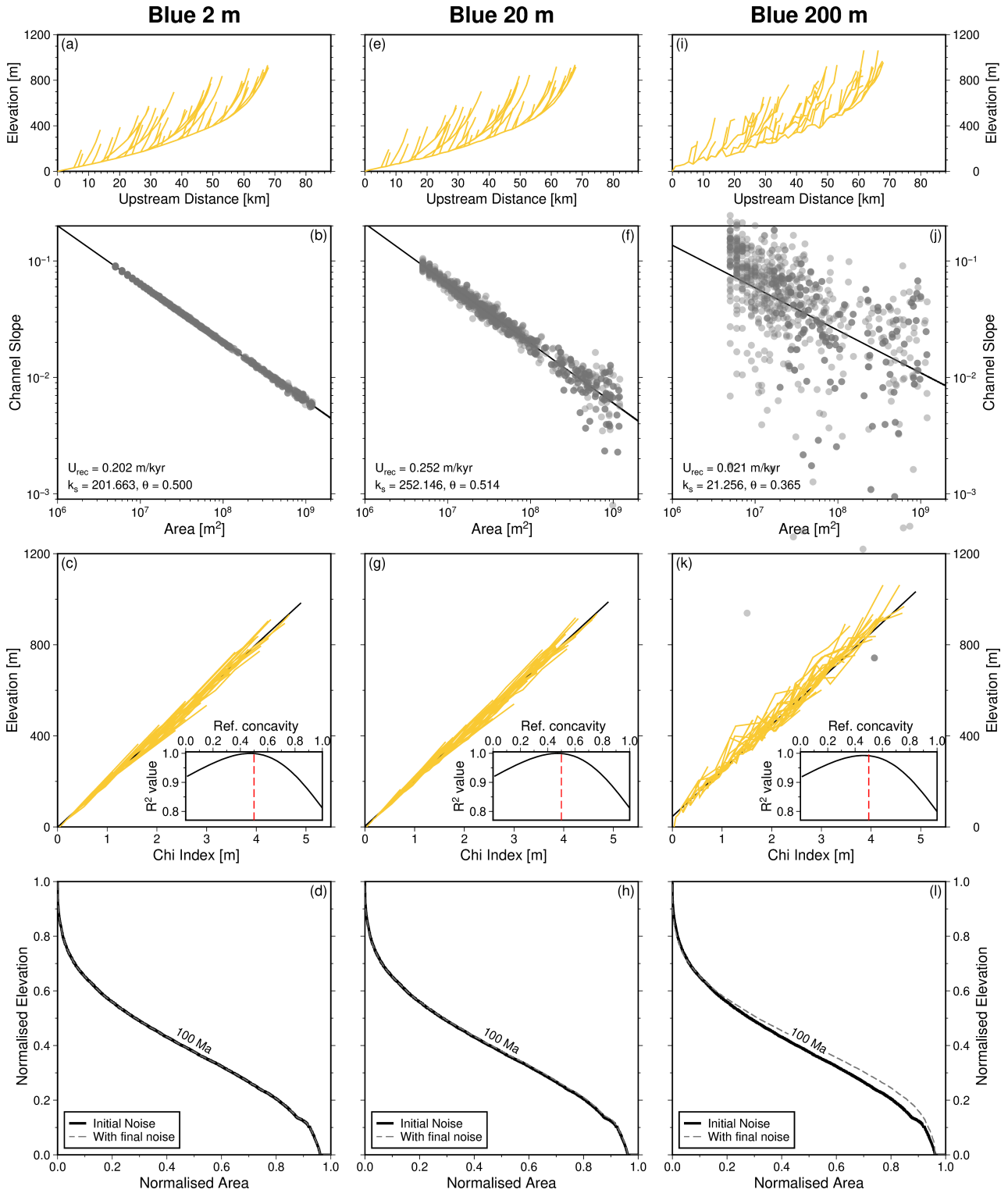


**Figure S11. Geometries of river profiles and associated metrics generated with un-eroded blue noise.** (a–j) See caption to Figure S9 for extended description.